Comparison of Short-Readout Trajectories for Diffusion-Weighted Imaging

S. J. Holdsworth[1], S. Skare[1], R. D. Newbould[1], A. Nordell[2], and R. Bammer[1]

[1]Department of Radiology, Stanford University, Palo Alto, CA, United States, [2]Hospital Physics, Karolinska University Hospital, Stockholm, Sweden

Introduction: "Short-Axis readout Propeller EPI" (SAP-EPI) (1), its dual-blade variant (dual-blade SAP-EPI) (2), and Readout-Segmented EPI (RS-EPI) (3) have been proposed as variants of EPI for high-resolution diffusion-weighted (DW) imaging. These "short-readout" (sr)-EPI readouts use a faster traversal of *k*-space and thus minimize artifacts from off-resonant spins and T_2^* decay resulting in significantly reduced distortions compared to single-shot EPI, particularly when used in combination with GRAPPA (1). There are a few intricacies of sr-EPI sampling strategies that may affect the scan efficiency and overall image quality. In addition to the requirement (or not) of an extra navigator, or the use of dual-readouts, the scan efficiency will also be dependant upon the diffusion preparation time. Thus, the purpose of this abstract is to assess these schemes with regard to diffusion preparation/acquisition ratio, normalized scan time, and image quality for a typical set of scan parameters we are using for high resolution GRAPPA (4-5)-accelerated DWI.

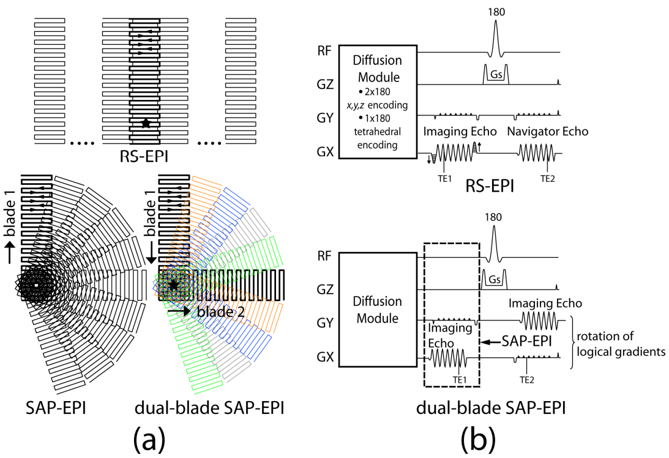

Figure 1. (a) RS-EPI, SAP-EPI, and dual SAP-EPI *k*-space trajectories. For all trajectories, the partial Fourier data are reconstructed with POCS (9-10) to fill in the remaining required extent of *k*-space. (b) sr-EPI pulse sequence diagrams following diffusion preparation module.

Materials & Methods: The three *k*-space trajectories and corresponding pulse sequence diagrams are shown in Fig. 1a and b, respectively. RS-EPI segments *k*-space into individual EPI 'blinds' along the readout direction, and requires an additional navigator blind (for phase correction of the DW blinds) acquired with the use of an additional refocusing pulse. SAP-EPI rotates individual 'blades' through the center of *k*-space, and does not require an extra navigator. For the dual-blade SAP-EPI method, a second 180° pulse is used to acquire a second blade, with the aim to achieve a shorter scan time. Striving for similar effective TE's between the two blades, the first and second half-Fourier blades are acquired inwards and outwards respectively from the *k*-space center. Experiments were conducted on a 1.5T whole-body MRI unit (GE Excite, G = 50mT/m, SLR = 150 mT/m/s) and an eight-channel head coil. To implement the RS-EPI sequence, our existing dual-blade SAP-EPI readout was modified such that the second echo served as a navigator, and with the imaging echoes acquired in an adjacent fashion. T2w (b = 0) and DW datasets were acquired on human volunteers using all proposed sr-EPI variants using the following diffusion preparation schemes: 1) Twice-refocusing with standard *x,y,z* diffusion encoding (or DTI), and 2) Stejskal-Tanner diffusion preparation with tetrahedral encoding (which minimizes the TE for a given b-value). A typical set of scan parameters that we have been using for high-resolution GRAPPA-accelerated DW sr-EPI imaging were used: a blade width of 64, a fixed target resolution of 288 x 288, a GRAPPA-acceleration factor R = 3, Partial Fourier encoding with 18 overscans, a slice thickness of 5 mm, TR = 3 s, a FOV = 26 cm, and a b-value of 1000 s/mm^2. RS-EPI used 5 blinds, SAP-EPI used 6 blades, and dual-blade SAP-EPI 3 orthogonal blades. Three repetitions of each sequence were conducted, each of which were phase corrected using a triangular windowing approach (6). The SNR efficiency as a function of SNR/sqrt(sequence time x blades) was obtained by taking the relative standard deviation over the mean of the three repeated b = 0 scans. The SNR was calculated as 1/mean(noise maps). A new distortion correction method based on the Reversed Gradient Polarity method (7,8) was applied to the SAP-EPI acquisitions. With this method, the ΔB_0 field was estimated on (and applied to) the SAP-EPI blades, without the need for collecting additional data.

Results: The minimum TEs achieved for both sequences are shown in Table 1. T2w images and noise maps with the corresponding SNR values for each sr-EPI diffusion preparation scheme are in Fig. 2. While the SAP-EPI and dual-blade SAP-EPI images presented have been corrected for distortion, the noise maps are calculated from the SAP-EPI variants *without* correction. Fig. 3 shows sr-EPI isotropic DW images from the dataset acquired with twice-refocusing.

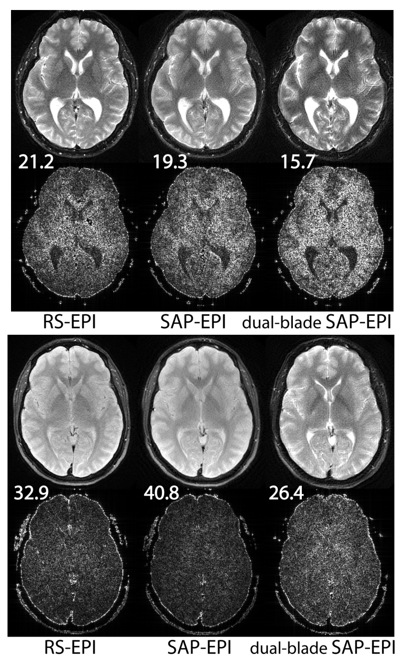

Figure 2. (top) One b = 0 image selected from each sr-EPI dataset acquired using a *twice refocused diffusion preparation and x,y,z encoding* (b = 1000 s/mm^2) and corresponding noise maps below. The numbers displayed for each image are the normalized SNR values. For the SAP-EPI variants, the images displayed have been corrected for distortion. (bottom) As above, acquired instead using a *Stejskal-Tanner diffusion preparation and tetrahedral encoding.*

Discussion & Conclusion: As given by the SNR values and noise maps in Fig. 2, dual-blade SAP-EPI is shown to be less effective than originally anticipated, despite the acquisition of an extra imaging blade per TR. Given our choice of parameters and hardware, the longer TE's (and late ending of the second blade) of dual-blade SAP-EPI, combined with the reduced number of slices that can be acquired per TR seems to result in a disadvantage with respect to SNR and T2 blurring. However, the properties of the second echo may need to be investigated further due to possible phase inconsistencies of the 180º pulse. Comparing RS-EPI and SAP-EPI, a slightly higher SNR is achieved for RS-EPI in the twice-refocused approach with *x, y, z* diffusion encoding (Fig. 2a). This may be explained by the requirement for fewer blinds/blades to fill *k*-space in RS-EPI, despite that more slices/TR can be acquired for SAP-EPI. The reverse is true, however, with the use of the Stejskal-Tanner diffusion preparation with tetrahedral encoding (Fig. 2b). The reason for this difference may partly be attributed to blurring due to the non-Cartesian nature of SAP-EPI, but more likely to its increased acquisition/sequence time ratio. With regard to overall image quality, it can be observed in Figs. 2 and 3 that residual distortion in SAP-EPI results in blurring, which can limit the effective resolution. On the contrary, the unidirectional distortions in RS-EPI allow the image resolution to be increased further, while the effective resolution is only limited by T2 decay and scan time. In summary, the short-axis EPI variants SAP-EPI and RS-EPI should be selected depending upon the scan parameters and diffusion preparation used. Further work will include simulations to disentangle distortions, RF effects and T2-decay. While the effect of eddy currents is already minimized with the use of sr-EPI readouts, for any residual eddy currents we anticipate the use of the Stejskal-Tanner method in combination with eddy current correction.

Diffusion preparation & encoding	**Minimum TE**	
	RS-EPI & SAP-EPI	**dSAP-EPI (TE_1/TE_2)**
Twice refocused, *x,y,z* encoding	70 ms	108/119 ms
Single refocused, tetrahedral encoding	43 ms	76/92 ms

Table 1. Minimum echo times for the three sr-EPI variants for the diffusion preparation module used in the text.

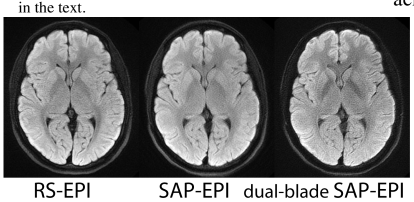

Figure 3. Isotropic sr-EPI DWI images (b =1000 s/mm^2, twice-refocusing, tetrahedral encoding) acquired at a target resolution of 288 x 288.

References: 1) Skare S. MRM 2006;55:1298-1307. 2) S Skare, ISMRM Arizona, 2007 3) Porter D et al. ISMRM 2004;442. 4) Griswold MA. et al. MRM 2002;47:1202-1210. 5) Qu P. et al. JMR 2005;174(1):60-67. 6) Pipe JG. MRM 1999;42(5):963-969. 7) Andersson JL. Neuroimage 2003;20(2):870-888. 8) Skare S. MRM 2005;54(1):169-181. 9) Haacke EM et al. JMR 1991;92:126-145. 10) Liang ZP et al. Rev MRM 1992;4:67-185.

Acknowledgements: This work was supported in part by the NIH (2R01EB002711, 1R21EB006860), the Center of Advanced MR Technology at Stanford (P41RR09784), Lucas Foundation, the Oak Foundation, and the Swedish Research Council (K2007-53P-20322-01-4).